

## Supporting Information

### Constructing Sn(II) doped $\text{SrNb}_2\text{O}_6$ for visible light response $\text{H}_2$ and $\text{O}_2$ evolution from water

Shuaishuai Liu,<sup>a</sup> Peng Li,<sup>\*a</sup> Wei Zhou,<sup>b</sup> Naoto Umezawa<sup>\*c</sup> and Guoxiu Wang<sup>d</sup>

a. Jiangsu Key Laboratory of Electrochemical Energy Storage Technologies, Department of Applied Chemistry, College of Materials Science and Technology, Nanjing University of Aeronautics and Astronautics, Nanjing 211100, P. R. China.

b. Department of Physics, Tianjin University, 92 Weijin Road, Nankai District, Tianjin, P. R. China.

c. Semiconductor R&D Center, Samsung Electronics, 1, Samsungjeonja-ro, Hwaseong-si, Gyeonggi-do 18448 Korea.

d. Center for Clean Energy Technology, School of Mathematical and Physical Sciences, Faculty of Science, University of Technology Sydney, Sydney NSW 2007, Australia.

## **Experimental Section**

### **Photocatalyst preparation**

Both of  $\text{SrNb}_2\text{O}_6$  and Sn(II) doped  $\text{SrNb}_2\text{O}_6$  samples were synthesized via a standard solid state reaction.  $\text{SrCO}_3$ (99.9%, Wako Pure Chemical Industries, Japan),  $\text{SnCl}_2$ (99.9%, Wako Pure Chemical Industries, Japan), and  $\text{Nb}_2\text{O}_5 \cdot n\text{H}_2\text{O}$  (70.6%  $\text{Nb}_2\text{O}_5$ , Mitsuwa Chemicals Co., Japan) were used as the starting reagents. To prepare  $\text{SrNb}_2\text{O}_6$  and Sn(II) doped  $\text{SrNb}_2\text{O}_6$ , the stoichiometrically mixed powder reagents were grinded in the present of 95% ethanol solution until a dry powder was obtained. Then, the grinded mixture was vacuum treated at 200°C for 10 hours to remove the adsorbed  $\text{O}_2$  and  $\text{H}_2\text{O}$ . Next, the mixture was calcined at 800°C for 10 hours in the atmosphere of Ar. After that, the powder was grinded, pressed into a pallet, and calcined at 1000°C for another 20 hours in the atmosphere of Ar to obtain the final products.

### **Photocatalyst characterization**

The crystal structures of the samples were determined with an X-ray diffractometer (X'Pert Powder, PANalytical B.V., Netherlands) with  $\text{Cu-K}\alpha$  radiation. The diffuse reflection spectra were measured with an integrating sphere equipped UV–visible recording spectrophotometer (UV-2600, Shimadzu Co., Japan) using  $\text{BaSO}_4$  as a reference and the optical absorption spectra were obtained by converting the reflection spectra using Kubelka-Munk equation. Scanning electron microscopy images were recorded with a field emission scanning electron microscopy (JSM-6701F, JEOL Co., Japan) operated at 15 kV. The specific surface areas were determined with a surface-

area analyzer (BEL Sorp-II mini, BEL Japan Co., Japan) by the Brunauer–Emmett–Teller (BET) method.

### **Photocatalytic H<sub>2</sub> and O<sub>2</sub> evolution experiments**

The H<sub>2</sub> evolution experiments were carried out in a gas-closed circulation system. The catalyst powder (0.3 g) was dispersed by using a magnetic stirrer in CH<sub>3</sub>OH aqueous solution (220 mL of distilled water + 50 mL of CH<sub>3</sub>OH) in Pyrex cell with a side window. Calculated amount of H<sub>2</sub>PtCl<sub>6</sub> solution (0.5 wt%) was added into the solution. The light source was a 300 W of Xe arc lamp ( $\lambda > 300$  nm). After irradiated for 3 hours, an L42 filter ( $\lambda > 400$  nm) was added to the Xe lamp to measure the visible light performance. The H<sub>2</sub> evolution was measured with an on-line gas chromatograph (GC-8A, Shimadzu) with a thermal conductivity detector (TCD) according to the standard curve.

The O<sub>2</sub> evolution experiments were carried out in the same system as H<sub>2</sub> evolution. The catalyst powder (0.3 g) was dispersed by using a magnetic stirrer in AgNO<sub>3</sub> aqueous solution (270 mL of distilled water + 3 mmol of AgNO<sub>3</sub>) in Pyrex cell with a side window. The light source was a 300 W of Xe arc lamp with an L42 cut-off filter ( $\lambda > 400$  nm). The O<sub>2</sub> evolution was measured with an on-line gas chromatograph (GC-8A, Shimadzu) with a thermal conductivity detector (TCD) according to the standard curve.

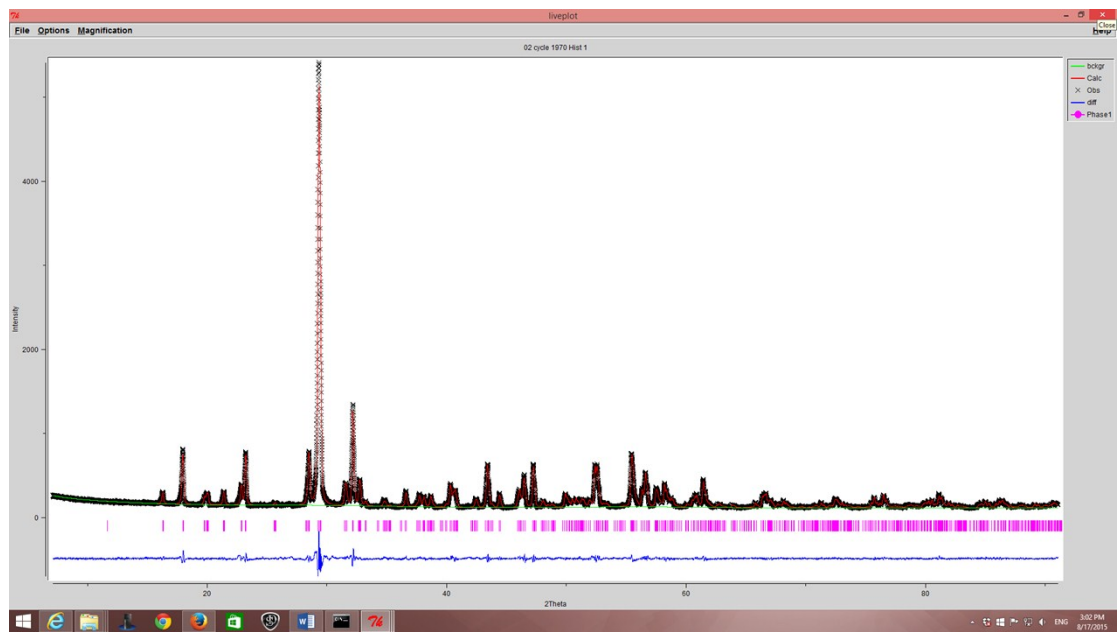
### **Theoretical calculation**

All calculations were performed with the Vienna ab-initio Simulation Package (VASP) based on the density functional theory (DFT). The Projector-augmented wave

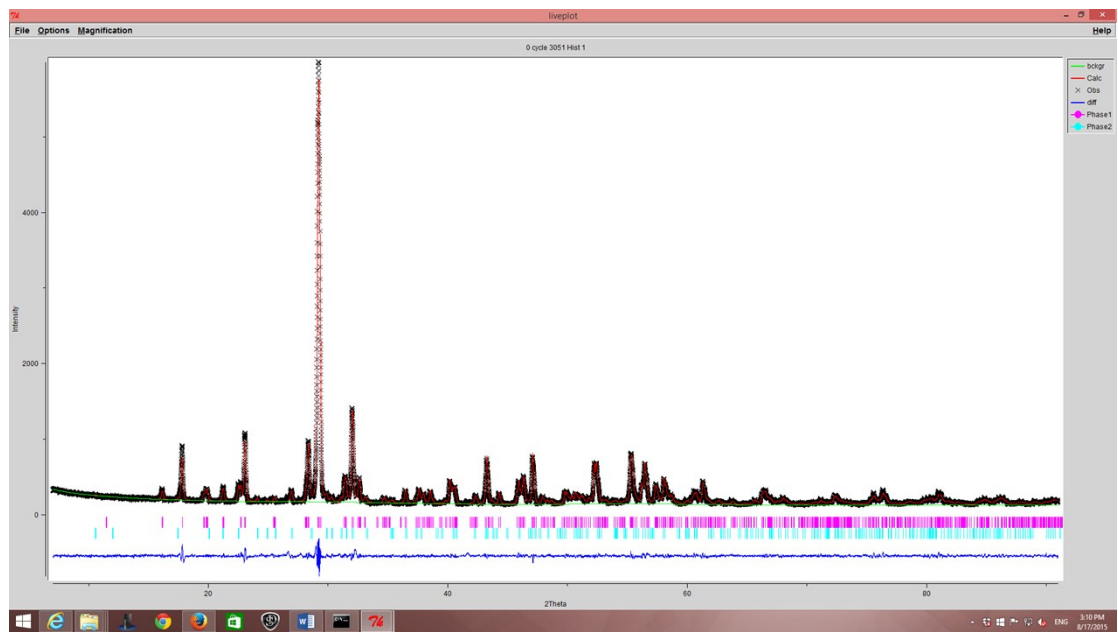
(PAW) was used for the electron-ion interactions. The HSE06 hybrid-functional with a mixing parameter of  $a = 0.25$  were employed to evaluate the exchange-correlation energy. The number of k points and the cut-off energy were increased until the calculated total energy converged within an error of  $1 \times 10^{-5}$  eV/atom. Therefore, the cut-off energy of 500 eV with  $3 \times 2 \times 2$  k points was set for the  $1 \times 2 \times 1$  supercell. The energy convergence tolerance was set to below  $5 \times 10^{-6}$  eV/atom. The lattice vectors and atomic coordinates were relaxed until the Hellmann-Feynman force on each atom is reduced to less than 0.01 eV/Å.

SI-1 The refined crystal XRD patterns.

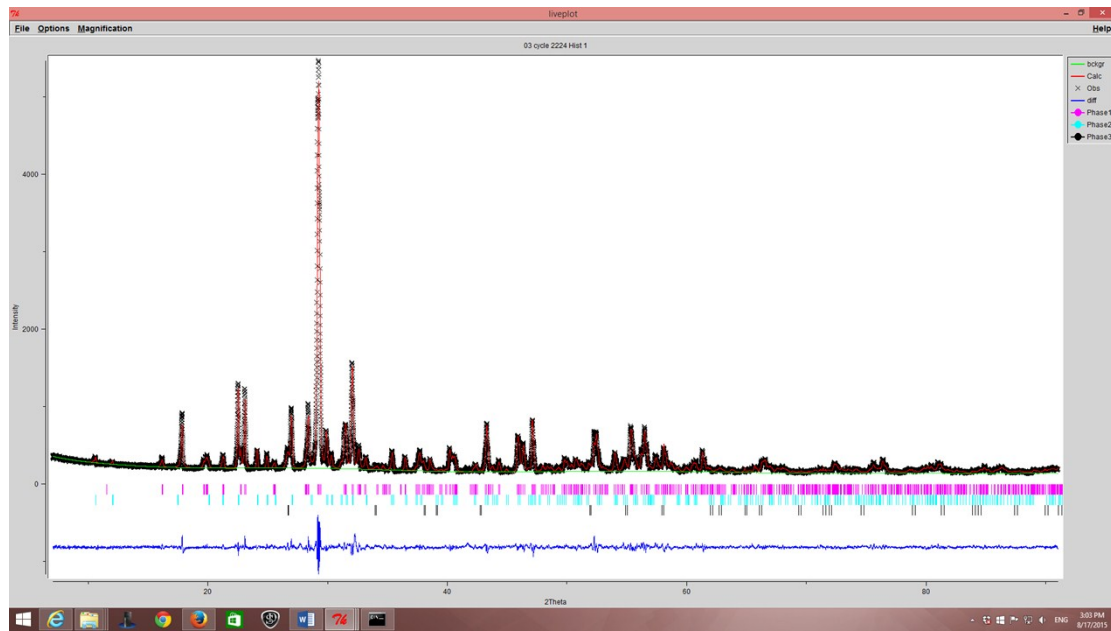
1. 10Sn-SrNb<sub>2</sub>O<sub>6</sub>



2. 20Sn-SrNb<sub>2</sub>O<sub>6</sub>



### 3. $30\text{Sn-SrNb}_2\text{O}_6$



SI-2 The refined crystal structures and lattice parameters of Sn doped SrNb<sub>2</sub>O<sub>6</sub>

	Lattice parameters						
	a (Å)	b (Å)	c (Å)	V(Å <sup>3</sup> )	$\alpha$ (°)	$\beta$ (°)	$\gamma$ (°)
SrNb <sub>2</sub> O <sub>6</sub> <sup>a</sup>	7.7291(1)	5.5991(1)	11.0059(1)	476.28(1)	90.00	90.36(1)	90.00
10Sn-SrNb <sub>2</sub> O <sub>6</sub> <sup>b</sup>	7.7282(2)	5.5971(1)	11.0006(2)	475.83(2)	90.00	90.36(1)	90.00
20Sn-SrNb <sub>2</sub> O <sub>6</sub> <sup>c</sup>	7.7223(2)	5.5946(1)	10.9943(2)	474.98(1)	90.00	90.36(1)	90.00
30Sn-SrNb <sub>2</sub> O <sub>6</sub> <sup>d</sup>	7.7267(2)	5.5964(1)	11.0017(2)	475.73(2)	90.00	90.35(1)	90.00
SrNb <sub>2</sub> O <sub>6</sub> <sup>e</sup>	7.6675	5.5744	10.9981	470.08	90.00	90.32	90.00
12.5Sn-SrNb <sub>2</sub> O <sub>6</sub> <sup>e</sup>	7.6460	5.5650	11.0105	468.49	90.01	90.32	90.00

<sup>a</sup> wRp = 0.0457, Rp = 0.0350

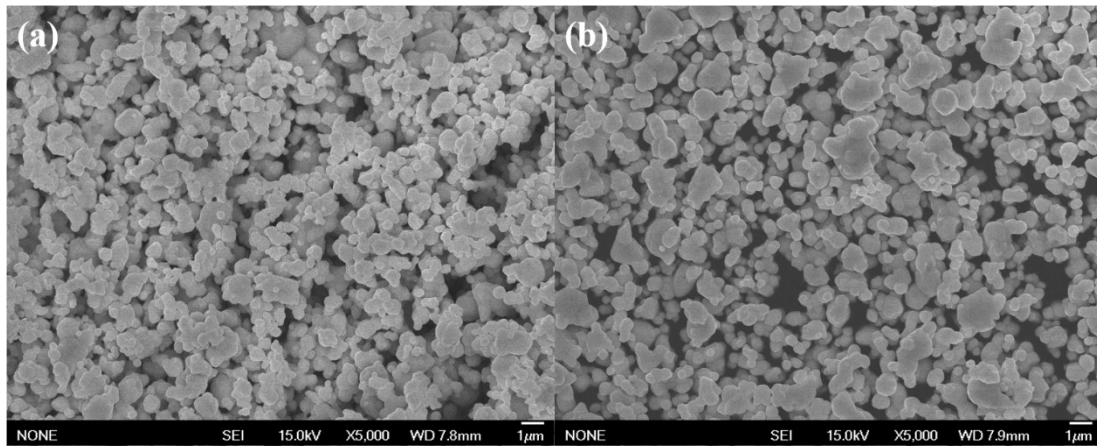
<sup>b</sup> wRp = 0.0498, Rp = 0.0377

<sup>c</sup> wRp = 0.0477, Rp = 0.0370

<sup>d</sup> wRp = 0.0621, Rp = 0.0477

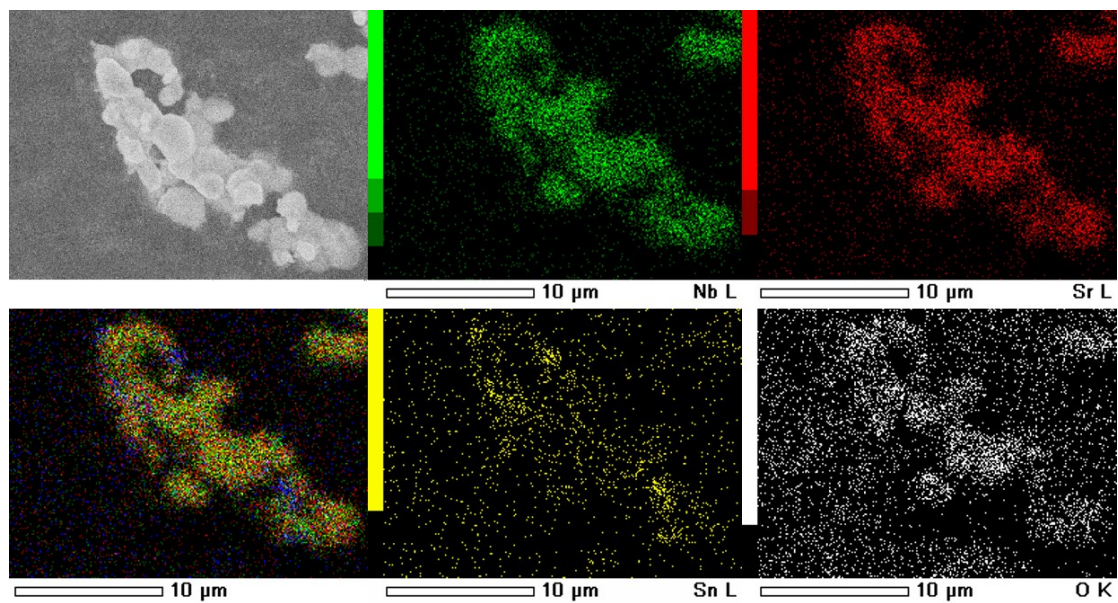
<sup>e</sup> From DFT optimization

SI-3 SEM images of the as-prepared (a)  $\text{SrNb}_2\text{O}_6$  and (b)  $20\text{Sn-SrNb}_2\text{O}_6$ .





SI-4 SEM mapping images of the as-prepared 20Sn-SrNb<sub>2</sub>O<sub>6</sub> sample.



Element	Nb	Sr	Sn	O
atom%	21.0	8.34	1.86	68.1

SI-5 The photophysical and photocatalytic properties of SrNb<sub>2</sub>O<sub>6</sub> and Sn(II) doped SrNb<sub>2</sub>O<sub>6</sub>

	Surface Area (m <sup>2</sup> ·g <sup>-1</sup> )	Optical band gap (eV)	H <sub>2</sub> evolution rate (μmol·h <sup>-1</sup> )
SrNb <sub>2</sub> O <sub>6</sub>	3.24	4.18	0
10Sn-SrNb <sub>2</sub> O <sub>6</sub>	3.47	2.67	10.8
20Sn-SrNb <sub>2</sub> O <sub>6</sub>	3.54	2.63	14.1
30Sn-SrNb <sub>2</sub> O <sub>6</sub>	3.61	2.61	13.3

SI-6 Sn 3d XPS spectra of the as-prepared Sn(II) doped SrNb<sub>2</sub>O<sub>6</sub> compared with SnO and SnO<sub>2</sub>.

